Geomechanics and Engineering, *Vol. 33, No. 5 (2023) 487-506*
https://doi.org/10.12989/gae.2023.33.5.487

Estimation of the soil liquefaction potential through the Krill Herd algorithm

Yetis Bulent Sonmezer[a] and Ersin Korkmaz*

Department of Civil Engineering, Engineering Faculty, Kirikkale University, 71451 Kirikkale, Turkey

(*Received Augsut 21, 2021, Revised February 14, 2023, Accepted April 23, 2023*)

Abstract. Looking from the past to the present, the earthquakes can be said to be type of disaster with most casualties among natural disasters. Soil liquefaction, which occurs under repeated loads such as earthquakes, plays a major role in these casualties. In this study, analytical equation models were developed to predict the probability of occurrence of soil liquefaction. In this context, the parameters effective in liquefaction were determined out of 170 data sets taken from the real field conditions of past earthquakes, using WEKA decision tree. Linear, Exponential, Power and Quadratic models have been developed based on the identified earthquake and ground parameters using Krill Herd algorithm. The Exponential model, among the models including the magnitude of the earthquake, fine grain ratio, effective stress, standard penetration test impact number and maximum ground acceleration parameters, gave the most successful results in predicting the fields with and without the occurrence of liquefaction. This proposed model enables the researchers to predict the liquefaction potential of the soil in advance according to different earthquake scenarios. In this context, measures can be realized in regions with the high potential of liquefaction and these measures can significantly reduce the casualties in the event of a new earthquake.

Keywords: earthquake; Krill Herd algorithm; optimization; soil liquefaction; structural damage

1. Introduction

Earthquake hazards can be categorized as soil liquefaction, seismicity, structural hazards, retaining structure failures, landslides, tsunamis, and pipeline hazards. Liquefaction caused by the seismic triggering of the ground is the main cause of damage to superstructures, infrastructures and pipeline systems as well as loss of life. Liquefaction occurs as a result of loss of strength in water-saturated loose sand layers due to the increase in pore water pressure under cyclic loading such as earthquakes. The phenomenon of soil liquefaction, described as the sudden loss of strength of loose sand layers, was known by Terzaghi *et al.* (1996) in the early stages of the development of soil mechanics. Although the phenomenon of soil liquefaction has been known for a long time, several devastating earthquakes around the world (Niigata and Alaska 1964, Loma Prieta 1989, Kobe 1995, Kocaeli 1999 and Chi-Chi 1999) have attracted the attention of the scientific community.

Researchers have put forth various approaches in the last few decades to comprehend the liquefaction mechanism and assess the liquefaction potential of soils. These techniques can be categorized into three primary classes (Green 2001) These three types of techniques are stress-based, deformation-based, and energy-based. The stress-based approach is the approach among these that is most frequently employed (Seed and Idriss 1971, Whitman 1971). It is frequently updated with new research and is typically based on empirical data from field observations and laboratory studies (e.g., Youd *et al.* 2001, Cetin *et al.* 2004). The number of cycles and the shear stress level serve as the method's primary criteria. The equivalent stress and cycle count are determined in the method put forth by Seed and Idriss (1971) in order to link the motion of a real earthquake to the harmonic loading conditions in a laboratory. Dobry *et al.* (1982) first suggested the unit deformation-based approach. It is generated from the dynamics of two idealized sand grains interacting, and it is then applied to natural soils (Green 2001, Baziara and Jafarian 2007, Alavi ve Gandomi 2012). This method is primarily based on the idea that, regardless of the kind of sand, relative density, starting effective stress value, or sample preparation technique, pore water pressure starts to build when the threshold shear strain value surpasses the value given as roughly 0.01%.

In order to evaluate the soil's potential for liquefaction, the energy-based technique was initially put forth as an alternative to the stress-based approach in the 1970s (Nemat-Nasser and Shokooh 1979). Since then, it has continued to be improved (Berrill and Davis 1985, Figueroa *et al*. 1994, Green 2001, Kokusho 2013). With or without liquefaction, in this method, the creation of additional pore water pressure is directly connected to the accumulation of energy per unit volume throughout the loading phase. The area within the hysteresis loop formed throughout a cycle is defined as the energy stored in a unit volume (J/m^3) associated with the permanent rearrangement of its particles. Since the energy of liquefaction is entirely reliant on the applied shear stress and shear strain, using unit energy to assess liquefaction makes sense (Fardad Aminia and Noorzad 2018). In actuality, the goal of all these techniques is to identify the soil variables that contribute to

*Corresponding author, Assistant Professor
E-mail: ersinkorkmaz@kku.edu.tr
[a]Associate Professor

ISSN: 2005-307X (Print), 2092-6219 (Online)

liquefaction and to illustrate their potential implications. The following summarizes a few studies on this topic.

Okur and Umu (2013) conducted a total of 52 resonant column and dynamic torsional shear tests in undrained conditions to comprehend the behavior of partially saturated sands and provide a general framework. The findings showed that the relative density, saturation rate, and confining stress all affect the cyclic strength of sand, and that partially saturated soils with saturation ratios Sr <60% are safer against cyclic stress brought on by matrix suction. In addition, Eseller-Bayat *et al*. (2019) carried out stress-controlled cyclic simple shear experiments to further investigate the combined effects of plasticity index (PI), fines content (FC), relative density (DR), and cyclic stress ratio (CSR) on sand samples with silt or clay content up to 10%. The findings demonstrated that when the packing index control parameter was chosen as DR, satisfactory trends were obtained for sands with low fines content. Moreover, compared to fine-grained sands up to 10% FC, samples of clean sand demonstrated the strongest liquefaction strength. As FC rises and CSR falls in somewhat denser samples, the impact of fine grains' plasticity is visible.

Hoque *et al.* (2017) looked at how saturated sands' resistance to liquefaction was affected by relative density and initial effective confining pressure. Undrained cyclic triaxial tests on two distinct sands at various relative densities and confining pressures were carried out in the lab for this purpose. The findings demonstrated that a rise in relative density led to an increase in CSR, which strengthened the soil's resistance to liquefaction. Additionally, they claimed that at low effective confining strains as opposed to relatively greater effective confining stresses, soils are more resistant to liquefaction. Moreover, Zhang *et al.* (2016) looked into the impacts of initial saturation degree, relative density, and effective confining pressure on the liquefaction resistance of unsaturated sands. The findings demonstrated that when saturation levels decreased, relative density and effective confining stress increased, so did the unsaturated sands' resistance to liquefaction. Additionally, was demonstrated that at 100% saturation degree, the influence of saturation degree on liquefaction resistance is more pronounced.

In addition to the laboratory tests mentioned above, soil liquefaction was also investigated by analytical studies. In these studies, prediction models were developed using data obtained from real field results. Some of these are summarized below. Muduli and Das (2014) performed a liquefaction analysis on SPT results using the simplified method proposed by Seed and Idriss (1971). (Xue and Xiao 2016, Xue and Yang 2016) developed a new model for the estimation of the soil liquefaction potential based on a hybrid genetic algorithm (GA) model, which relies on particle swarm optimization, and the support vector machine (SVM) technique. Some analytical studies on soil liquefaction in the literature are given briefly.

Hanna *et al.* (2007) proposed a neural network regression model to determine the soil liquefaction potential using 620 data sets obtained from the earthquakes in Turkey and Taiwan (1999). They used 12 ground and seismic parameters in their modeling. The proposed GRNN model predicted accurately the occurrence of soil liquefaction at the sites where the data were obtained. In addition, Baziar and Jafarian (2007) created an artificial neural network (ANN) model to determine the relationship between soil starting properties and the strain energy necessary to produce liquefaction in sands and silty sands. They used a sizable dataset of 284 previously published findings of cyclic triaxial, torsional shear, and simple shear tests to build the model. In assessing the liquefaction resistance (capacity energy) of soils using the idea of strain energy, the suggested model produced very positive findings. Ardakani and Kohestani (2015) used the C4.5 decision tree algorithm to estimate the seismic liquefaction potential of the soil based on the Cone Penetration Test (CPT) data. The results of the C4.5 decision tree were compared with the results from the existing artificial neural network (ANN) and relevance vector machine (RVM) models. They stated that the overall classification success rate for the whole data set was 98%.

Hu *et al.* (2016) developed a prediction model for soil liquefaction using two different Bayesian network theorems. Generally, they stated that both models performed well. They also carried out sensitivity analysis on input factors. They reported that among the twelve variables, the vertical effective stress, standard penetration test number, soil type, depth of soil deposit, and peak ground acceleration had more important effects on soil liquefaction. Moreover, Javdanian *et al.* (2017) used the neuro-fuzzy group method of data handling (GMDH) algorithm and optimization technique to determine the strain energy required for liquefaction. In the study, they developed a liquefaction energy estimation model using the parameters of effective stress, relative stiffness, D_{50}, C_u (uniformity coefficient), C_c (coefficient of curvature) and fine particle ratio. They stated that the model, proposed based on the laboratory results, can be successfully used for estimating the liquefaction potential based on strain energy.

Sabbar *et al.* (2019) used Artificial neural network (ANN) and genetic programming methods to estimate and develop the ratio of the minimum deviatoric stress to the initial peak deviatoric stress (qmin / qpeak), which is accepted as the static liquefaction criterion for clean sandy soils. The findings of this study showed that there is a good agreement between ANN and symbolic regression in predicting the qmin/qpeak ratio based on laboratory tests. In addition Ghorbani and Eslami (2021) created a thorough, energy-based model for evaluating the liquefaction potential of various varieties of sandy soils, including clear, silty, and clayey sands. A history of 100 examples from around the world with different soil qualities has been used to successfully validate the model. The findings demonstrated that the present model is vastly superior to earlier energy-based models.

The present study, the development of soil liquefaction prediction models in different forms and performance comparisons were made using the Krill Herd algorithm. For this purpose, among the 12 parameters obtained from the database case records of Cetin *et al*. (2016) and Seed *et al.* (1985), the 5 priority parameters in liquefaction (earthquake

magnitude, fine grain ratio, effective stress, corrected standard penetration test blow count and maximum ground acceleration) determined. Linear, Exponential, Power and Quadratic models were developed according to these determined parameters. Exponential model gave more accurate results than other models. Suggested model;

• It is easier, faster and more advantageous than other models in determining the liquefaction potential of sandy soils.

• The parameters used can be easily determined from field conditions and seismic hazard analysis.

• It gives very accurate results in estimating case outcomes.

2. Krill Herd algorithm

There is a tendency for herding in shrimps, which is common to most of the living beings. Although flocks of thousands of shrimp appear to be random formations from the outside, this action actually develops systematically Hofmann *et al.* (2004).

The shrimp flock, which disperse during an attack, aims to create a herd again and find food after the danger passes. In this context, shrimp individuals move towards the highest density and the best solution available for food. The Krill Herd (KH) algorithm was developed by Gandomi and Alavi (2012) by modeling this process. The advantages of the krill herd algorithm such as the easy application, robust structure, and being controlled by less parameters increase its competitive power against the other effective algorithms. This algorithm, whose popularity and usage area is increasing day by day, has shown successful results in different engineering problems such as economic load dispatch, color image multilevel thresholding segmentation, wireless sensor network, radial distribution system and structural seismic reliability evaluation (Mandal *et al.* 2014, Sultana and Roy 2016, Asteris *et al.* 2019, Karthick and Palanisamy 2019, He and Huang 2020).

The KH consists of a combination of each krill movement. At this stage, we can see that each krill has a function, and the herd is a combination of these functions. The functions of the individuals depend on 3 basic parameters:

- Movement induced by other krill individuals
- Foraging activity
- Random diffusion

Based on these 3 parameters, the Lagrangian model is generalized to an n-dimensional decision space as given in Eq. (1).

$$\frac{dX_i}{dt} = N_i + F_i + D_i \tag{1}$$

where N_i is the motion induced by other krill individuals; F_i is the foraging motion, and D_i is the physical diffusion of the ith krill individuals.

➢ *Motion induced by other krill individuals*

The krill individuals try to maintain a high density and move due to their mutual effects. Therefore, the direction of motion-induced is determined based on the local swarm, target swarm, and repulsive swarm densities. This movement is defined in Eq. (2).

$$N_i^{new} = N^{max} a_i + \omega_n N_i^{old} \tag{2}$$

$$a_i = a_i^{local} + a_i^{target} \tag{3}$$

N^{max} is the maximum triggered speed. $\omega_n$is the inertial weight of the triggered motion in the range [0,1] and N_i^{old} is the last motion triggered. The local influence of the krills adjacent to the ith krill is a_i^{local} and the best krill movement is defined as a_i^{target}. a_i^{local} is regarded as a repulsive and attractive effect of the local neighboring krills. The effect of the neighbor kril individuals is defined as in Eq. (4)

$$a_i^{local} = \sum_{j=1}^{NN} \hat{K}_{i,j} \hat{X}_{i,j} \tag{4}$$

$$\hat{X}_{i,j} = \frac{X_j - X_i}{\|X_j - X_i\| + \varepsilon} \tag{5}$$

$$\hat{K}_{i,j} = \frac{K_i - K_j}{K^{worst} - K^{best}} \tag{6}$$

where K^{worst} and K^{best} are the worst and the best fitness values of the krill individuals; K_i represents the fitness value of the ith krill individual; K_j is the fitness of jth (j = 1,2,. . .,NN) neighbor; X represents the related positions; and NN is the number of the neighbors.

Sensing distance ($d_{s,i}$) is calculated according to Eq. (7) in KH algorithm

$$d_{s,i} = \frac{1}{5N} \sum_{j=1}^{N} \|X_i - X_j\| \tag{7}$$

In the herd, the distance of the ith krill to each individual is checked and the neighborhood status of the krill is evaluated. Neighboring krills affect each other both positively and negatively. The expression leading to the global optima point is given in Eq. (8)

$$a_i^{target} = C^{best} \hat{K}_{i,best} \hat{X}_{i,best} \tag{8}$$

$$C^{best} = 2\left(rand + \frac{I}{I_{max}}\right) \tag{9}$$

Here, $rand$ parameter is a value in the range of 0-1 to increase the accuracy of the optimization; I is the number of iterations and I_{max} is the maximum number of iterations.

➢ *Foraging motion*

Foraging action is determined by two main parameters. These are the place of the food and previous experiences. Foraging movement is expressed by Eq. (10)

$$F_i = V_f \beta_i + \omega_f F_i^{old} \tag{10}$$

$$\beta_i = \beta_i^{food} + \beta_i^{best} \tag{11}$$

where V_f is the foraging rate; ω_f is the inertial weight of the foraging move in the range [0,1]; F_i^{old} is the last foraging move. β_i is a value that depends on β_i^{food}, which is the attractiveness of the food and β_i^{best}, which is the best target function ever.

The effect of the food is defined by its location. The location of the food must be calculated first, and then the attractiveness of the food. The place of the food is recalculated after each iteration from Eq. (12)

$$X^{food} = \frac{\sum_{i=1}^{N} \frac{1}{K_i} X_i}{\sum_{i=1}^{N} \frac{1}{K_i}} \tag{12}$$

$$\beta_i^{food} = C^{food} \hat{K}_{i,food} \hat{X}_{i,food} \tag{13}$$

$$C^{food} = 2\left(1 - \frac{I}{I_{max}}\right) \tag{14}$$

$$\beta_i^{best} = \hat{K}_{i,ibest} \hat{X}_{i,ibest} \tag{15}$$

Where, C^{food} is the food coefficient and K_{ibest} is the best previously visited position of the ith krill individual.

➢ *Physical diffusion*

The random diffusion motion of krill individuals depends on the diffusion rate and the direction of movement. Maximum diffusion speed is given in Eq. (16)

$$D_i = D^{maks}\delta \tag{16}$$

where D^{maks} is the maximum diffusion rate and δ is the direction of motion.

➢ *Motion process of the KH algorithm*

The described movements generally work to optimize the position of each krill individual. The position vector of a krill is formulated as in Eq. (17) when a time duration of Δt passes from a specific moment t

$$X_i(t + \Delta t) = X_i(t) + \Delta t \frac{dX_i}{dt} \tag{17}$$

$$\Delta t = C_t \sum_{j=1}^{NV} \left(UB_j - LB_j\right) \tag{18}$$

where NV is the total number of variables, UB_j and LB_j are the upper and lower limiting values, respectively, C_t corresponds to an empirical value in the range of [0,2].

➢ *Steps of the Krill Herd Algorithm*

I. Data structures: Algorithm parameters, determination of boundaries etc.
II. Initiation: Randomization of the first population in the search area.
III. Conformity Assessment: Assessment of krill individuals according to their positions
IV. Motion Calculation:
- Movement triggered by other individuals
- Foraging movement
- Random spread motion

V. Crossing and Application of Mutation
VI. Update: Updating the location of individuals in the search area
VII. Repeat: Go back to step III until the stop condition is met.
VIII. Finish

3. Development of the model

Models in different forms, used for prediction of soil liquefaction, have been developed by using the krill swarm algorithm. A total of 170 data, belonging to K. Ö nder Ç etin and Harry Bolton Seed, were used as the data set. Of the 170 data, 153 of them were randomly allocated for the study, and 17 as test data. These data are given in Appendix 1. In the development stage of the models, the most effective parameters among 12 parameters related to the earthquake and soil were determined through the J48 decision tree of WEKA Hall *et al.* (2009). The decision tree structure in WEKA is shown in Fig. 1. Parameters in this data set are the earthquake magnitude (M_w), peak ground acceleration (a_{max}), average depth (D_{avg}), groundwater table depth (D_{GWT}), total stress (σ), effective stress (σ'), average raw standard penetration test (SPT) blow count (N_{avg}), adjusted SPT blow count ($N_{(1)60}$), fines grain content (FC), clean sand corrected SPT blow count ($(N1)_{60CS}$), overload correction factor (K_σ) and relative density (D_r)

In the decision tree given in Fig. 1, values of 1 represent states with liquefaction and values of 0 represent states without liquefaction. The fact that the value of $N_{(1)60}$ is at the top of the decision tree shows that $N_{1(60)}$ is the most effective parameter in liquefaction among the 12 parameters analyzed. There is a total of 50 data with $N_{1(60)}$ value greater than 21.1. While there was no liquefaction in 44 of these data, liquefaction occurred in 6 of them. In other words, by just looking at the $N_{1(60)}$ value, liquefaction prediction can be made with an accuracy rate of 88%, depending on whether this value is less than or greater than 21.1. In this case, we can say that the most obvious criterion in this data group is the $N_{1(60)}$value, since the liquefaction estimation is so high by looking at only one parameter.

For cases where $N_{1(60)}$ value is less than 21.1 value, Mw parameter should be checked. For M_w, the magnitude value of 6.54 is distinctive, but M_w is not a decisive parameter on its own. Other parameters should be considered, depending on whether the magnitude of the earthquake is smaller or larger than this value. In cases where M_w is less than 6.54, the a_{max} value is decisive. There are 28 cases where a_{max} is less than 0.19. Liquefaction was observed in only 1 of these cases. When this order is continued by looking at the decision tree, it is seen that the σ' and FC are also effective parameters in liquefaction, in order of importance. For this

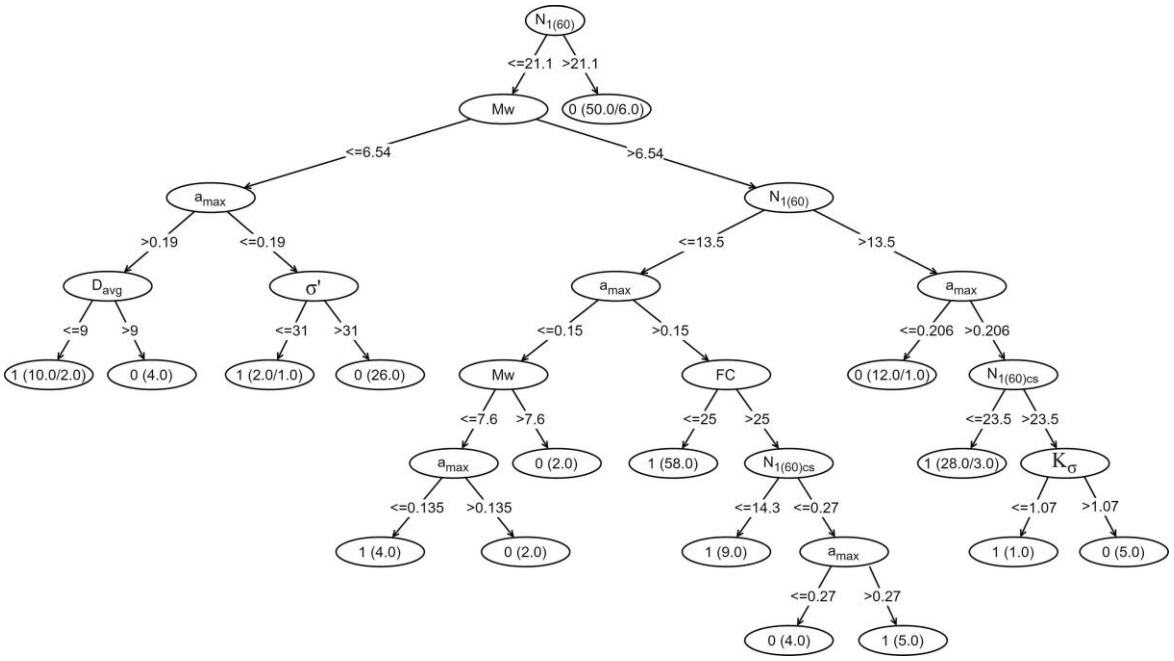

Fig. 1 WEKA Decision Tree

Table 1 Parameters of the Study

Earthquake magnitude	M_w
Peak ground acceleration	a_{max}
Effective stress	σ'
Modified SPT blow count	$N_{1(60)}$
Fines Content	FC

reason, the M_w , a_{max} , σ', $N_{1(60)}$ and FC parameters determined from the decision tree and given in Table 1 during the development of the models were used in the study.

However, this should not be forgotten. Recent studies have shown that parameters such as the coefficient of uniformity (C_u), average grain diameter (D_{50}) and plasticity index (PI), which are effective in liquefaction, are also important in determining the liquefaction potential of the soil (Eseller *et al.* 2019, Sonmezer *et al* 2020, Monkul *et al.* 2021). It is clear that more accurate results can be obtained with the use of more input parameters. However, the proposed model gives very successful results in determining the liquefaction potential of sandy soils with less input parameters with high accuracy. In this proposed model, it is very fast and efficient to determine the liquefaction potential by estimating possible earthquake parameters (M_w and a_{max}) in an area and knowing the SPT test result, which can be easily done everywhere, and knowing only the fine grain content (FC) of the sandy soil.

Among the five most important parameters affecting soil liquefaction, two parameters were established to be related to the earthquake intensity (a_{max} ve M_w) and the others to soil behavior ($N_{1(60)}$, σ', FC). The first key parameter responsible for soil liquefaction is the $N_{1(60)}$ value, which essentially characterizes the soil behavior and is obtained from SPT. For plotting and interpreting the field data, Bolton Seed *et al.* (1985) proposed the use of $N_{1(60)}$, which represents the driving energy of the drill rod equal to 60% of the theoretical free-fall energy in the SPT test. The second key parameter is the earthquake magnitude (M_w), which is a measure of the energy generated during the earthquake. In addition, the maximum horizontal ground acceleration (a_{max}) measured at the ground surface, which depends on the magnitude of the earthquake and the characteristics of the soil layers, is prominent in characterizing the liquefaction behavior Cetin *et al.* (2004). Bolton Seed *et al.* (1985) adopted the use of FC value, commonly corresponding to the critical depth, in liquefaction analysis. Xenaki and Athanasopoulos (2003) showed that the liquefaction resistance of sandy silt mixes decreased as the non-plastic FC increased to 35% and 44%, and then the resistance started to increase. Effective stress (σ') is another important parameter affecting soil behavior. Lee and Seed (1967) and Figueroa et al. (1994) stated in their experimental studies that the liquefaction potential of the soil decreases with the increase of σ' and this potential increases with the decrease of σ'. Since the intervals of each parameter value are different from each other, the parameter values should be normalized in developing the model according to the determined parameters. Linear normalization was applied to normalize the parameters to the range of [0,1]. Normalization graphs are shown in Figs. 2-6 and curve equations are shown in Eqs. (19)-(23).

In this study, liquefaction estimation models were developed in linear, power, exponential and quadratic model forms. The developed model forms are given in Eqs. (24)-(27)

- The effective stress normalization line equation

$$\sigma' = \frac{X - \sigma'_{min}}{\sigma'_{max} - \sigma'_{min}} = \frac{X - 20{,}00}{171{,}00 - 20{,}00} \qquad (19)$$

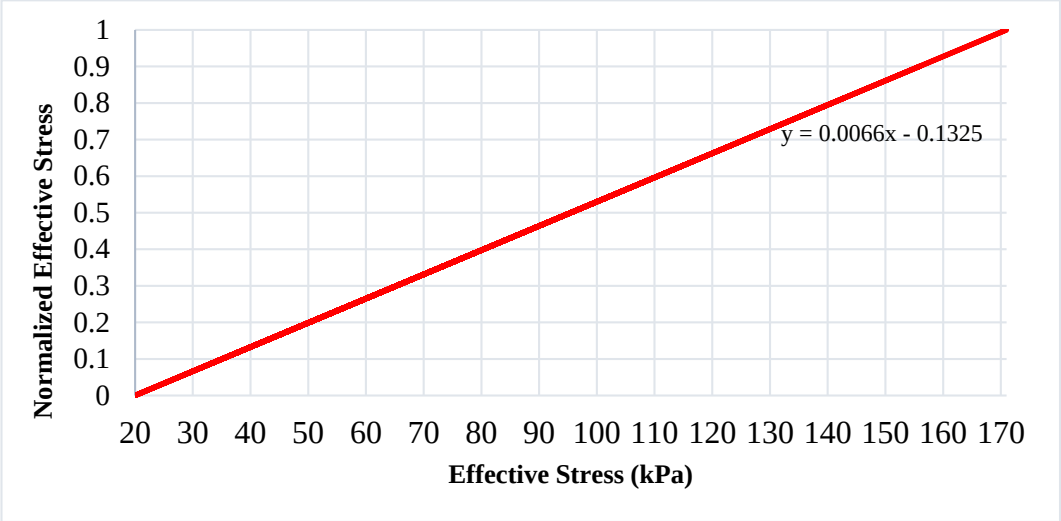

Fig. 2 Effective Stress Normalization Graph

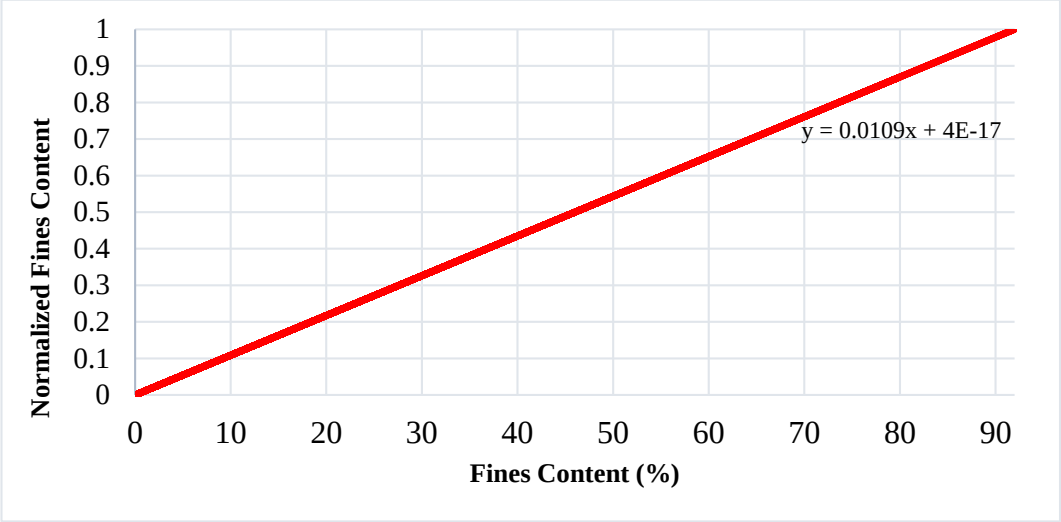

Fig. 3 Fines Content Normalization Graph

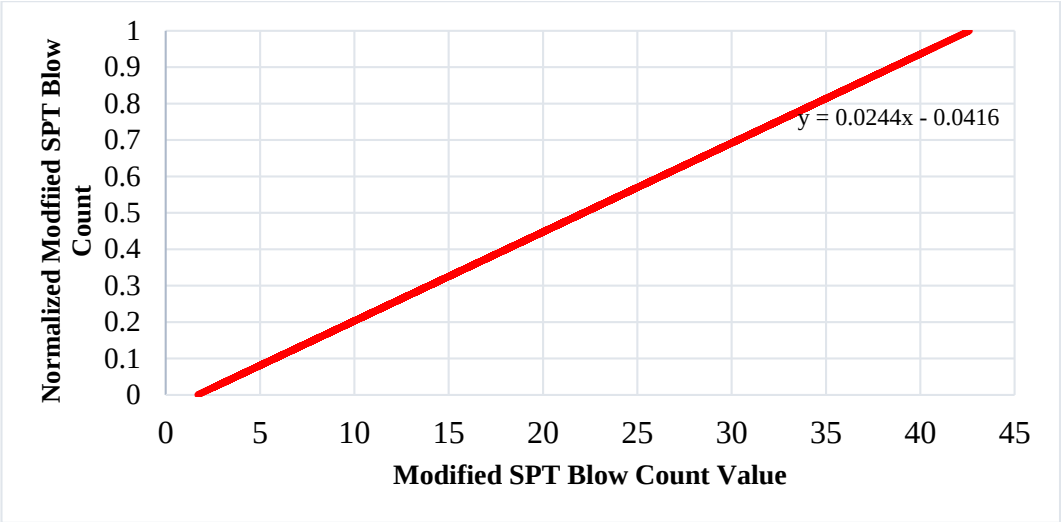

Fig. 4 Modified SPT Blow Count Normalization Graph

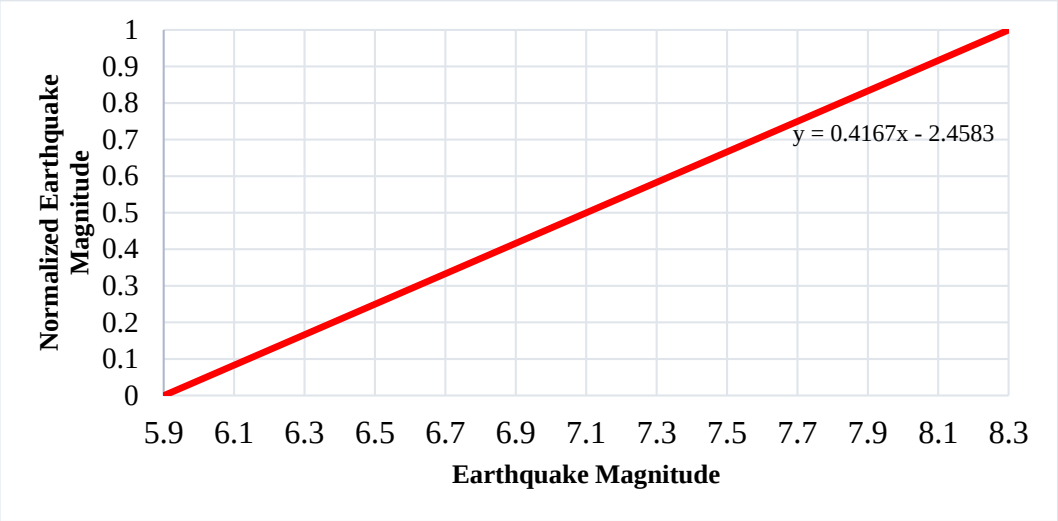

Fig. 5 Earthquake Magnitude Normalization Graph

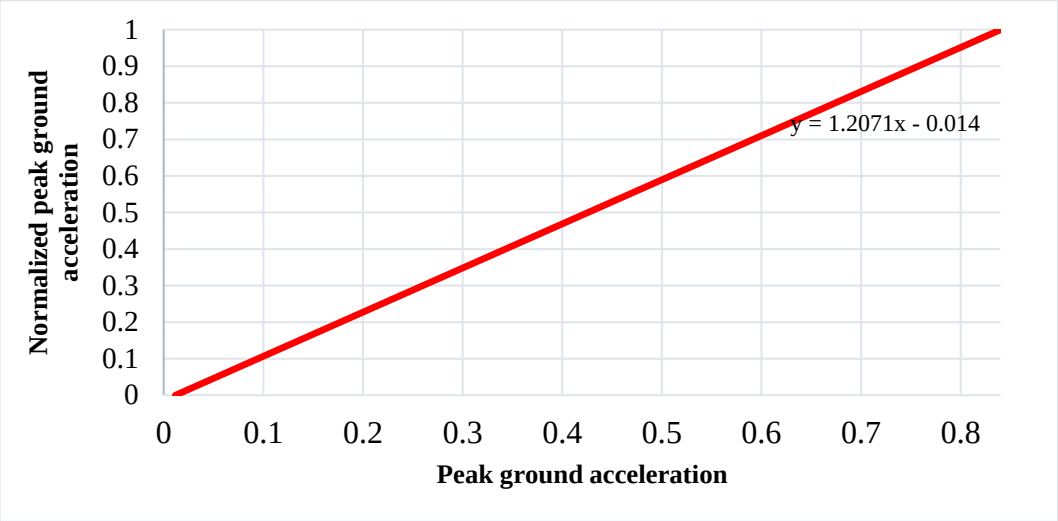

Fig. 6 Peak ground acceleration normalization graph

- The fines content normalization line equation

$$FC = \frac{X - FC_{min}}{FC_{max} - FC_{min}} = \frac{X - 0{,}00}{92{,}00 - 0{,}00} \quad (20)$$

- Modified SPT blow count normalization line equation

$$N_{1(60)} = \frac{X - N_{1(60)_{min}}}{N_{1(60)_{max}} - N_{1(60)_{min}}} = \frac{X - 1{,}70}{42{,}60 - 1{,}70} \quad (21)$$

- Earthquake magnitude normalization line equation

$$M_w = \frac{X - M_{w_{min}}}{M_{w_{max}} - M_{w_{min}}} = \frac{X - 5{,}90}{8{,}30 - 5{,}90} \quad (22)$$

- Peak ground acceleration normalization line equation

$$a_{max} = \frac{X - a_{max_{min}}}{a_{max_{max}} - a_{max_{min}}} = \frac{X - 0{,}01}{0{,}84 - 0{,}01} \quad (23)$$

- Linear Model

$$Lm = M_w * X_1 + FC * X_2 + \sigma' * X_3 + N_{1(60)} * X_4 + a_{max} * X_5 + X_6 \quad (24)$$

- Power Model

$$Pm = X_1 * {M_w}^{X_2} + X_3 * FC^{X_4} + X_5 * {\sigma'}^{X_6} + X_7 * {N_{1(60)}}^{X_8} + X_9 * {a_{max}}^{X_{10}} + X_{11} \quad (25)$$

- Exponential Model

$$Em = X_1 * e^{X_2 M_w} + X_3 * e^{X_4 FC} + X_5 * e^{X_6 \sigma'} + X_7 * e^{X_8 N_{1(60)}} + X_9 * e^{X_{10} a_{max}} + X_{10} \quad (26)$$

- Quadratic Model

$$Qm = X_1 * {M_w}^2 + X_2 * FC^2 + X_3 * \sigma'^2 + X_4 * {N_{1(60)}}^2 + X_5 * {a_{max}}^2 + X_6 * M_w * FC + X_7 * M_w * \sigma' + X_8 * M_w * N_{1(60)} + X_9 * M_w * a_{max} + X_{10} * FC * \sigma' + X_{11} * FC * N_{1(60)} + X_{12} * FC * a_{max} + X_{13} * \sigma' * N_{1(60)} + X_{14} * \sigma' * a_{max} + X_{15} * N_{1(60)} * a_{max} + X_{16} \quad (27)$$

X(i): The coefficients in the models.

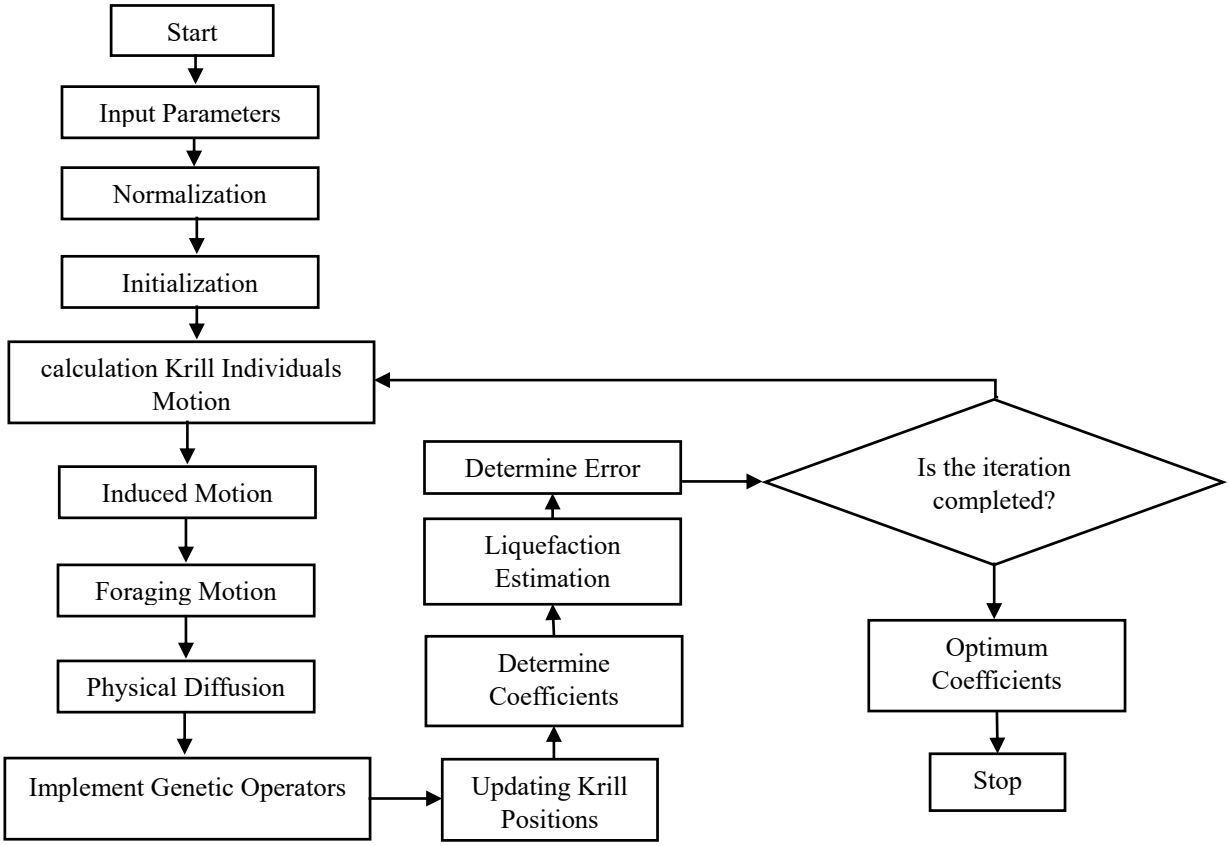

Fig. 7 Application Flow Diagram

Table 2 Confusion Matrix

Liquefaction		Estimation	
		Liquefaction Presence	Liquefaction Absence
Observed	Liquefaction Presence	TP	FN
	Liquefaction Absence	FP	TN

Table 3 Control Parameters

N^{max}	0.01 ms^{-1}
V_f	0.02 ms^{-1}
D^{max}	0.005 ms^{-1}
NR	10
NP	50
MI	200

There are two values in the target function of this study. These are 0 for no liquefaction and unity for liquefaction. It is necessary to compare the results of the prediction equation with the related values under real field conditions. The confusion model in Table 2 is used for comparison and this method is widely preferred to measure the margin of error for such problems Townsend (1971).

The parameters TN, FP, FN and TP, which are initially 0, are determined for each case. The accuracy margin in Eq. (28) is obtained from the ratio of correctly predicted values (TP and TN) to the sum of all predictions (TN, FP, FN, TP). The target function used in the development of the models was created to maximize the accuracy between the liquefaction state estimated from the krill herd algorithm and the actual liquefaction state, and this expression is given in Eq. (28).

$$Accuracy = \frac{TP + TN}{TN + FP + FN + TP} \tag{28}$$

$$Max\ F(x) = \sum_{n=1}^{m} Accuracy \tag{29}$$

In the development of soil liquefaction prediction models, the model coefficients were determined by the krill-herd algorithm, and the flow diagram is shown in Fig. 7.

4. Results and discussion

The coefficients of the developed equations were determined by the krill herd algorithm. The efficiency of the optimization is directly related to the control parameters of the algorithm. The control parameters of the krill herd algorithm are foraging rate (V_f), maximum spread rate (D_{max}), maximum triggered speed (N^{max}), number of studies (NR) and number of krill individuals (NP). (Gandomi and

Table 4 Coefficients of models

Linear		Power		Exponential		Quadratic	
X_1	-19.7211	X_1	0.3348	X_1	0.3628	X_1	0.3175
X_2	-12.0702	X_2	2.7774	X_2	-2.6107	X_2	6.1337
X_3	-2.8668	X_3	6.0306	X_3	2.4415	X_3	-1.6634
X_4	-33.2797	X_4	8.4426	X_4	-8.3024	X_4	-5.5637
X_5	-5.1492	X_5	-4.3872	X_5	-0.7755	X_5	-1.0923
		X_6	5.4676	X_6	-3.2958	X_6	-0.8671
		X_7	-9.2018	X_7	16.3484	X_7	8.8557
		X_8	1.1616	X_8	-1.6305	X_8	-13.0112
		X_9	3.5144	X_9	-9.1869	X_9	16.5599
		X_{10}	0.4783	X_{10}	-8.6516	X_{10}	-0.5163
		X_{11}	-3.0475	X_{11}	0.2941	X_{11}	-7.3640
						X_{12}	-2.0410
						X_{13}	-3.0497
						X_{14}	-4.4425
						X_{15}	-0.6327
						X_{16}	1.8898

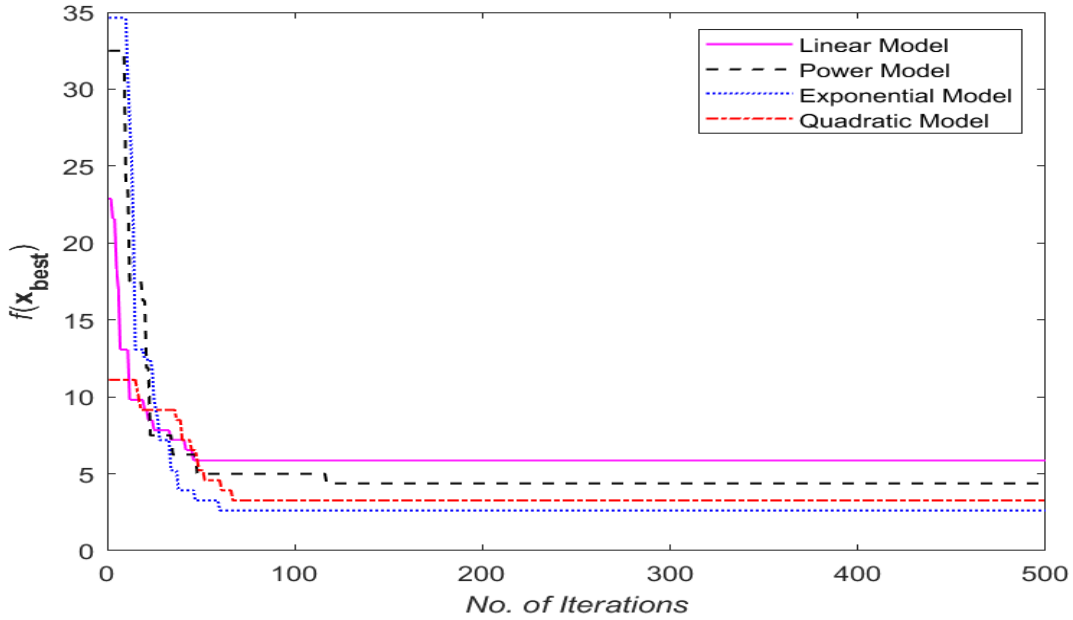

Fig. 8 Krill Herd Algorithm Performance Graph

Alavi 2012) compared the performance of different control parameter values and suggested optimum values. The control parameter values used in this study were selected according to the recommended optimum values and are given in Table 3.

The model multipliers obtained from the krill herd algorithm for the developed models are shown in Table 4. Performance charts of the krill herd algorithm are shown in Fig. 8. The values in the figure are the percent error values of the models. When Fig. 8 is examined, the minimum error value can be seen to be reached within the first 60 iterations in linear, power and quadratic models, and in the first 117 iterations in the power model. Percentage errors and accuracies of the training and test data used in the

Table 5 The Percent Error and Accuracy Values for the Training and Test Data

		Linear	Power	Exponential	Quadratic
Training	Errors (%)	5.88	4.37	2.61	3.27
	Accuracy (%)	94.12	95.63	97.39	96.23
Test	Errors (%)	23.52	23.52	11.76	11.76
	Accuracy (%)	76.47	76.47	88.24	88.24

Table 6 Liquefaction Predictions for the Test Data

	Linear		Power		Exponential		Quadratic	
Observe Liq.	Estimate Liq.	Normalize Value	Estimate Liq.	Normalize Value	Estimate Liq.	Normalize Value	Estimate Liq.	Normalize Value
0	0	0	0	0.10	0	0.00	0	0.00
1	1	0.86	1	0.63	1	1.00	1	0.89
1	1	0.84	1	0.63	1	0.85	1	0.80
1	1	0.82	1	0.67	1	0.70	1	0.86
1	1	0.72	1	0.85	1	0.68	1	0.92
1	1	0.78	1	1.00	1	0.74	1	0.87
1	1	1	1	0.67	1	0.72	1	0.76
0	1	0.56	0	0.38	0	0.09	0	0.48
0	1	0.59	0	0.00	0	0.06	1	0.53
0	1	0.67	0	0.41	0	0.24	1	0.57
1	0	0.46	0	0.49	0	0.42	1	0.67
1	1	0.57	0	0.49	1	0.57	1	0.92
1	1	0.57	0	0.47	1	0.63	1	1.00
1	1	0.51	1	0.58	1	0.54	1	0.85
1	1	0.96	0	0.42	0	0.46	1	0.55
1	1	0.61	1	0.51	1	0.64	1	0.78
1	1	0.59	1	0.52	1	0.63	1	0.67

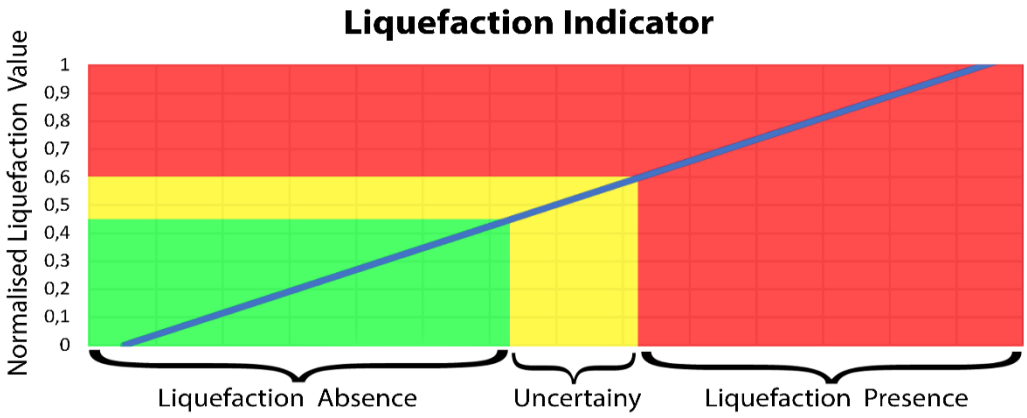

Fig. 9 Soil Liquefaction Prediction Graph

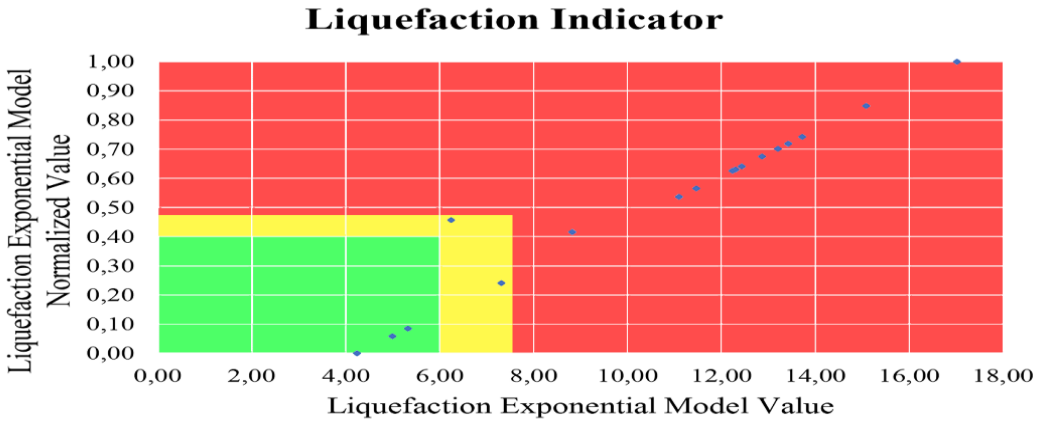

Fig. 10 Liquefaction Prediction Graph of the Exponential Model

Table 7 Liquefaction Predictions for the Validation Data

					Linear		**Power**		**Exponential**		**Quadratic**	
Observed Liq.	Ghorbani and Eslami (2021)	Baziar and Jafarian (2007)	Davis and Berril (1982)	Trifunac (1985)	Est. Liq.	Norm. Value	Est. Liq.	Norm. Value	Est. Liq.	Norm. Value	Est. Liq.	Norm. Value
1	1	0	1	1	1	0,53	0	0,40	1	0,54	1	0,62
1	1	0	1	1	1	0,51	0	0,42	0	0,47	1	0,56
1	1	0	1	1	1	0,58	1	0,66	1	0,79	1	0,80
1	1	0	1	1	1	0,59	1	0,66	1	0,78	1	0,76
1	1	0	1	1	1	0,60	1	0,67	1	0,84	1	0,79
1	1	0	1	1	1	0,60	1	0,62	1	0,75	1	0,74
1	1	0	1	1	0	0,49	0	0,39	0	0,48	1	0,55
0	0	0	0	0	1	0,58	0	0,41	0	0,46	1	0,61
0	1	0	1	1	1	0,58	0	0,38	0	0,47	1	0,62
1	1	0	1	1	1	0,55	0	0,47	1	0,59	1	0,66
0	0	0	1	1	1	0,55	0	0,42	0	0,49	1	0,64
1	1	0	1	1	1	0,58	1	0,68	1	0,70	1	0,63
0	1	0	1	1	0	0,43	0	0,38	0	0,41	0	0,41
1	1	0	1	1	1	0,55	1	0,59	1	0,59	1	0,57
1	1	0	1	1	1	0,52	1	0,54	1	0,56	1	0,59
0	1	0	1	1	0	0,43	0	0,38	0	0,41	0	0,44
0	0	0	1	1	0	0,24	0	0,16	0	0,28	0	0,21
1	1	0	1	1	0	0,50	1	0,51	1	0,55	1	0,60
0	1	0	1	1	0	0,37	0	0,30	0	0,37	0	0,39
0	0	0	1	1	0	0,27	0	0,19	0	0,31	0	0,27
1	1	0	1	1	1	0,54	0	0,50	1	0,53	1	0,55

development of the models are given in Table 5. In addition, the liquefaction prediction values for 17 test data are shown in Table 6. According to Table 5, exponential model showed the best performance with 2.61% error value. The worst model performance belongs to the linear model with 5.88% error value. As can be seen from Fig. 8, it has been observed that the KH algorithm yields successful results in liquefaction prediction models with the worst error of approximately 6% in a short iteration period.

The present study showed that the model with the highest accuracy among different model forms is the Exponential Model. It had an accuracy of 97.39% in training data and 88.24% in test data. According to the 17 estimation results given in Table 6, Exponential model made 2 wrong and 15 correct estimations. Accordingly, it has an accuracy of 88.24% with 15 correct predictions in 17 data. The statistics of the test data can be interpreted as low, since the number of test data is small and each false estimate has a statistical error of 5.88%. However, the statistical result in the training data and the very low number of false predictions among the test data reveal the validity and high level of accuracy of the model. The Quadratic model, on the other hand, showed the second-best performance, showing an accuracy of 96.23% in the training data and 2 wrong predictions in the test data. Power and linear models showed the worst performances with 95.63% and 94.12% accuracies, respectively. In addition, these models made 4 incorrect predictions in the test data.

The liquefaction prediction values (normalized values) of the models given in Table 6 were used to determine the liquefaction. For the validation of the models, 73 different validation data were used, excluding the study data. These data are given in Appendix 2. The proposed models were compared with 4 previous studies. The results of 73 data are given in Tablo 7. The accuracy and error rates of previous studies and proposed models for 73 data are given in Table 8. The linear model performed worse than the study in 2021 and showed better results than the other 3 studies. The power and quadratic models showed success close to the study conducted in 2021 and showed better results than the other 3 studies and the linear model. The best performing exponential model outperformed the previous 4 studies. Among the previous studies, the study by Ghorbani and Eslami in 2021 achieved 89.04% success with 8 incorrect predictions in 73 data, while the exponential model was able to predict liquefaction with an accuracy of 90.41% with 7 incorrect predictions.

The liquefaction state was determined as no liquefaction (0) when the normalized value is less than 0.5 and as liquefaction (1) when it is greater than 0.5. When the predictions of the models are examined according to the test data, it was seen that the erroneous predictions fall between 0.45 and 0.60, and this region was interpreted as the zone of uncertainty. Accordingly, the estimation results of the

Table 7 (continued)

					Linear		**Power**		**Exponential**		**Quadratic**	
Observed	Ghorbani and	Baziar and	Davis and	Trifunac	Est.	Norm.	Est.	Norm.	Est.	Norm.	Est.	Norm.
Liq.	Eslami (2021)	Jafarian (2007)	Berril (1982)	(1985)	Liq.	Value	Liq.	Value	Liq.	Value	Liq.	Value
0	0	0	1	0	0	0,12	0	0,00	0	0,19	0	0,00
1	1	0	1	1	1	0,57	1	0,52	1	0,53	1	0,60
1	1	0	1	1	1	0,54	0	0,50	1	0,53	1	0,55
0	0	0	1	0	0	0,12	0	0,00	0	0,19	0	0,00
1	1	0	1	1	1	0,52	1	0,53	0	0,48	1	0,51
1	1	0	1	1	1	0,70	1	0,64	1	0,76	1	0,78
1	1	0	1	1	1	0,58	1	0,69	1	0,66	1	0,65
1	1	0	1	1	1	0,56	1	0,61	1	0,55	1	0,59
0	0	0	1	1	0	0,49	0	0,39	0	0,34	0	0,43
1	1	0	1	1	1	0,59	1	0,59	1	0,64	1	0,66
1	1	0	1	1	1	0,55	1	0,51	1	0,56	1	0,60
1	1	0	1	1	1	0,70	1	0,64	1	0,76	1	0,78
1	1	0	1	1	1	0,58	1	0,69	1	0,66	1	0,65
1	1	0	1	1	1	0,52	1	0,54	1	0,51	1	0,55
1	1	0	1	1	1	0,53	1	0,56	1	0,53	1	0,55
0	1	0	1	1	0	0,50	0	0,48	0	0,43	1	0,50
1	1	0	1	1	1	0,56	1	0,61	1	0,55	1	0,59
0	0	0	1	0	0	0,15	0	0,10	0	0,21	0	0,11
0	0	0	1	1	0	0,49	0	0,39	0	0,34	0	0,43
0	0	0	1	1	0	0,34	0	0,25	0	0,25	0	0,28
0	0	0	1	1	0	0,34	0	0,25	0	0,26	0	0,28
1	1	0	1	1	1	0,58	1	0,68	1	0,65	1	0,64
0	0	0	1	1	0	0,31	0	0,23	0	0,24	0	0,25
1	1	0	1	1	1	0,96	1	0,64	1	0,93	1	0,97
0	1	1	1	1	0	0,10	1	0,88	0	0,17	1	0,57
0	1	1	1	1	0	0,12	1	0,92	0	0,29	1	0,62
1	1	0	1	1	1	0,58	1	1,00	1	0,69	1	0,59
1	1	0	1	1	1	0,61	0	0,47	1	0,63	1	0,71
1	1	0	1	1	1	0,52	0	0,39	0	0,47	1	0,53
1	1	0	1	0	0	0,48	0	0,35	0	0,48	1	0,48
1	1	0	1	1	1	0,63	1	0,66	1	0,66	1	0,70
1	1	0	1	1	1	0,64	1	0,90	1	1,00	1	0,77
1	1	0	1	1	1	0,65	1	0,50	1	0,64	1	0,58
1	1	0	1	1	1	0,66	1	0,68	1	0,70	1	0,76
0	0	0	0	0	1	0,50	0	0,36	0	0,37	1	0,53
0	1	0	1	1	0	0,00	0	0,46	0	0,00	0	0,37
1	1	0	1	1	1	0,61	0	0,44	1	0,55	1	0,68
0	0	0	1	0	0	0,45	0	0,50	0	0,38	0	0,45
0	0	0	1	1	1	0,57	1	0,63	0	0,50	1	0,55
1	1	0	1	0	1	0,86	0	0,48	1	0,74	1	0,92
1	1	0	0	0	1	0,97	1	0,50	1	0,81	1	1,00
1	1	0	0	0	1	0,85	1	0,58	1	0,87	1	0,98
1	1	0	0	0	1	0,83	1	0,53	1	0,79	1	0,93

Table 7 Continued-

					Linear		**Power**		**Exponential**		**Quadratic**	
Observed	Ghorbani and	Baziar and	Davis and	Trifunac	Est.	Norm.	Est.	Norm.	Est.	Norm.	Est.	Norm.
Liq.	Eslami (2021)	Jafarian (2007)	Berril (1982)	(1985)	Liq.	Value	Liq.	Value	Liq.	Value	Liq.	Value
1	1	0	0	0	1	0,87	0	0,50	1	0,76	1	0,93
1	1	0	0	0	1	0,85	1	0,51	1	0,76	1	0,92
1	1	0	0	0	1	0,82	0	0,48	1	0,70	1	0,88
1	1	0	1	0	1	0,57	0	0,44	0	0,49	1	0,65
1	1	0	1	0	1	0,81	1	0,52	1	0,76	1	0,91
1	1	0	0	0	1	0,83	0	0,48	1	0,70	1	0,88
1	1	0	0	0	1	0,93	0	0,46	1	0,73	1	0,94
1	1	0	0	0	1	0,87	0	0,48	1	0,73	1	0,91
1	1	0	1	1	0	0,46	0	0,35	0	0,47	1	0,47

Table 8 The Percent Error and Accuracy Values for the Validation Data

		Ghorbani and Eslami (2021)	Baziar and Jafarian (2007)	Davis and Berril (1982)	Trifunac (1985)	**Linear**	**Power**	**Exponential**	**Quadratic**
Validation	Errors (%)	10.96	71.23	41.10	41.10	28.77	12.33	9.59	10.96
	Accuracy (%)	89.04	28.77	58.90	58.90	71.23	87.67	90.41	89.04

models are divided into 3 parts and shown in Fig. 9. Liquefaction prediction graph of the Exponential model with the best performance is given in Fig. 10:

- If KHA <0,45, soil liquefaction is not expected according to the existing parameters. (The green shaded area in Fig. 10)
- If 0,45< KHA <0,60, the region of uncertainty shows that there is possibility of soil liquefaction and more parameters are needed for a more precise analysis. (The yellow shaded area in Fig. 10)
- If 0,60<KHA, soil liquefaction is certainly expected according to the existing parameters and the necessary precautions absolutely need to be taken. (The red shaded area in Fig. 10)

5. Conclusions

The number of studies carried out with the krill herd algorithm, both in its main form and with its hybridization with different methods, has been increasing every year since the algorithm was first published. The reason for this increase can be interpreted as the increasing confidence in a relatively new algorithm compared to other conventional optimization algorithms every year. The reason for the krill herd algorithm to be used in different areas is that it is a versatile algorithm. In this direction, the performance of the krill herd algorithm in the field of soil liquefaction was investigated for the first time in this study. In the study, soil liquefaction was tried to be predicted by using $M_w, a_{max}, \sigma', N_{1(60)}, FC$ parameters in krill herd algorithm approach. Following conclusions were drawn from the study:

- The weight coefficients of the equations were determined through the krill herd algorithm. The exponential model form reached the highest accuracy according to the training data. In addition, it has made the least wrong estimations among the test data.
- In the exponential model, the liquefaction prediction value (normalized value) is obtained in the range of 0-1. The domain for this value is interpreted as follows:
- If KHA <0,45, soil liquefaction is not expected according to the existing parameters.
- If 0,45< KHA <0,60, there is a possibility of soil liquefaction and the liquefaction should be investigated by using more parameters.
- If 0,60<KHA, liquefaction is certainly expected according to the available parameters. The necessary precautions need to be taken, absolutely.
- In this study, the performances of the equations created in linear, power, exponential and quadratic model forms were investigated. Among the equation forms established to determine the soil liquefaction, the exponential model gave the most accurate results, while the linear model gave the least accurate ones. Nevertheless, it has been demonstrated by statistical data that the linear model with the worst performance of approximately 5% error and other models can be used in the prediction of soil liquefaction.
- With this proposed model based on KH algorithm, soil liquefaction of a site can be easily determined from drilling studies ($\sigma', N_{1(60)}, FC$) and seismic hazard analysis (M_w, a_{max}) with 98% accuracy.

References

Alavi, A.H. and Gandomi, A.H. (2012), "Energy-based numerical models for assessment of soil liquefaction", *Geosci. Front.*, **3**(4), 541-555. https://doi.org/10.1016/j.gsf.2011.12.008.

Ardakani, A. and Kohestani, V.R. (2015), "Evaluation of liquefaction potential based on CPT results using C4. 5 decision tree", *J. AI Data Min.*, **3**(1), 85-92. http://dx.doi.org/10.5829/idosi.JAIDM.2015.03.01.09

Asteris, P.G., Nozhati, S., Nikoo, M. and Cavaleri, L. (2019), "Krill herd algorithm-based neural network in structural seismic reliability evaluation", *Mech. Adv. Mater. Struct.*, **26**(13), 1146-1153. https://doi.org/10.1080/15376494.2018.1430874.

Baziar, M.H. and Jafarian, Y. (2007), "Assessment of liquefaction triggering using strain energy concept and ANN model capacity energy" *Soil Dyn. Earthq. Eng.*, **27**(12), 1056-1072. https://doi.org/10.1016/j.soildyn.2007.03.007.

Berrill, J.B. and Davis, R.O. (1985), "Energy dissipation and seismic liquefaction of sands: revised model", *Soils Found.*, **25**(2), 106-118. https://doi.org/10.3208/sandf1972.25.2_106.

Bolton Seed, H., Tokimatsu, K., Harder, L.F. and Chung, R.M. (1985), "Influence of SPT procedures in soil liquefaction resistance evaluations", *J. Geotech. Eng.*, **111**(12), 1425-1445. https://doi.org/10.1061/(ASCE)0733-9410(1985)111:12(1425).

Cetin, K.O., Seed, R.B., Der Kiureghian, A., Tokimatsu, K., Harder Jr, L.F., Kayen, R.E. and Moss, R.E. (2004), "Standard penetration test-based probabilistic and deterministic assessment of seismic soil liquefaction potential", *J. Geotech. Geoenviron. Eng.*, **130**(12), 1314-1340. https://doi.org/10.1061/(ASCE)10900241(2004)130:12(1314).

Cetin, K.O., Seed, R.B., Kayen, R.E., Moss, R.E., Bilge, H.T., Ilgac, M. and Chowdhury, K. (2016), "Summary of SPT based field case history data of cetin (2016) database", METU/GTENG 08/16-01; Middle East Technical University.

Davis, R.O., Berrill, J.B. (1982), "Energy dissipation and seismic liquefaction in sands", *Earthq. Eng. Struct. D.*, **10**(1), 59-68. https://doi.org/10.1002/ eqe.4290100105.

Dobry, R., Ladd, R.S., Yokel, F.Y., Chung, R.M. and Powell, D. (1982), *Prediction of Pore Water Pressure Buildup and Liquefaction of Sands During Earthquakes by the Cyclic Strain Method*, **138**(150), Gaithersburg, MD: National Bureau of Standards.

Eseller-Bayat, E., Monkul, M.M, Akın, Ö. and Yenigun, S. (2019), "The coupled influence of relative density, CSR, plasticity and content of fines on cyclic liquefaction resistance of sands", *J. Earthq. Eng.*, **23**(6), 909-929. https://doi.org/10.1080/13632469.2017.1342297.

Fardad, A.P. and Noorzad, R. (2018), "Energy-based evaluation of liquefaction of fiber-reinforced sand using cyclic triaxial testing", *Soil Dyn. Earthq. Eng.*, **104,** 45-53. https://doi.org/10.1016/j.soildyn.2017.09.026.

Figueroa, J.L., Saada, A.S., Liang, L. and Dahisaria, N.M. (1994), "Evaluation of soil liquefaction by energy principles", *J.of Geotechnical Engineering*, **120**(9), 1554-1569. https://doi.org/10.1061/(ASCE)0733-9410(1994)120:9(1554)

Gandomi, A.H. and Alavi, A.H. (2012), "Krill herd: a new bio-inspired optimization algorithm", *Commun. Nonlinear Sci. Numer. Simul.*, **17**(12), 4831-4845. https://doi.org/10.1016/j.cnsns.2012.05.010.

Ghorbani, A. and Eslami, A. (2021), "Energy-based model for predicting liquefaction potential of sandy soils using evolutionary polynomial regression method", *Comput. Geotech.*, **129**, 103867.

Green, R.A. (2001), "Energy-based Evaluation and Remediation of Liquefiable Soils", PhD. Dissertation, Virginia Polytechnic Institute and State University, Blacksburg

Hall, M., Frank, E., Holmes, G., Pfahringer, B., Reutemann, P. and Witten, I.H. (2009), "The WEKA data mining software: an update", *ACM SIGKDD explorations newsletter*, **11**(1), 10-18.

Hanna, A.M., Ural, D. and Saygili, G. (2007), "Neural network model for liquefaction potential in soil deposits using Turkey and Taiwan earthquake data", *Soil Dyn. Earthq. Eng.*, **27**(6), 521-540. https://doi.org/10.1016/j.soildyn.2006.11.001.

He, L. and Huang, S. (2020), "An efficient krill herd algorithm for color image multilevel thresholding segmentation problem", *Appl. Soft Comput.*, **89**, 106063. https://doi.org/10.1016/j.asoc.2020.106063.

Hofmann, E.E., Haskell, A.E., Klinck, J.M. and Lascara, C.M. (2004), "Lagrangian modelling studies of Antarctic krill (Euphausia superba) swarm formation", *ICES J. Mar. Sci.*, **61**(4), 617-631. https://doi.org/10.1016/j.icesjms.2004.03.028.

Hoque, M.M., Ansary, M.A. and Yasin, S.J. (2017), "Effects of relative density and effective confining pressure on liquefaction resistance of sands" *Proceedings of the 19th International Conference on Soil Mechanics and Geotechnical Engineering*, Seoul, South Korea, September.

Hu, J.L., Tang, X.W. and Qiu, J.N. (2016), "Assessment of seismic liquefaction potential based on Bayesian network constructed from domain knowledge and history data", *Soil Dyn. Earthq. Eng.*, **89**, 49-60. https://doi.org/10.1016/j.soildyn.2016.07.007.

Javdanian, H., Heidari, A. and Kamgar, R. (2017), "Energy-based estimation of soil liquefaction potential using GMDH algorithm", *Iranian J. Sci. Tech. T.Civil Eng.*, **41**(3), 283-295. https://doi.org/10.1007/s40996-017-0061-4.

Karthick, P.T. and Palanisamy, C. (2019), "Optimized cluster head selection using krill herd algorithm for wireless sensor network", *Automatika: časopis za automatiku, mjerenje, elektroniku, računarstvo i komunikacije*, **60**(3), 340-348. https://doi.org/10.1080/00051144.2019.1637174.

Kokusho, T. (2013), "Liquefaction potential evaluation: energy-based method comparedto stress-based method", *Proceedings of the 7th International Conference on Case Histories in Geotechnical Engineering*, Chicago, USA, April.

Lee, K.L. and Seed, H.B. (1967), "Cyclic stress conditions causing liquefaction of sand", *J. Soil Mech. Found. Division*, **93**(1), 47-70.

Mandal, B., Roy, P.K. and Mandal, S. (2014), "Economic load dispatch using krill herd algorithm", *Int. J. Elec. Power Energy Syst.*, **57**, 1-10. https://doi.org/10.1016/j.ijepes.2013.11.016.

Monkul, M.M., Kendir, S.B., Tütüncü, Y.E. (2021), "Combined effect of fines content and uniformity coefficient on cyclic liquefaction resistance of silty sands", *Soil Dynamics and Earthquake Engineering*, **151**, 106999 https://doi.org/10.1016/j.soildyn.2021.106999

Muduli, P.K. and Das, S.K. (2014), "Evaluation of liquefaction potential of soil based on standard penetration test using multi-gene genetic programming model", *Acta Geophysica*, **62**(3), 529-543. https://doi.org/10.2478/s11600-013-0181-6.

Nemat-Nasser S. and Shokooh A. (1979), "A unified approach to densification and liquefaction of cohesionless sand in cyclic shearing", *Can. Geotech. J.*, **16**(4), 659-678. https://doi.org/10.1139/t79-076.

Okur, V. and Umu, S.U. (2013), "Energy approach to unsaturated cyclic strength of sand", *Bull Earthq. Eng.*, **11**, 503-519. https://doi.org/ 10.1007/s10518-012-9396-1.

Sabbar, A.S., Chegenizadeh, A. and Nikraz, H. (2019), "Prediction of liquefaction susceptibility of clean sandy soils using artificial intelligence techniques", *Indian Geotech. J.*, **49**(1), 58-69. https://doi.org/10.1007/s40098-017-0288-9.

Seed, H.B. and Idriss, I.M. (1971), "Simplified procedure for evaluating soil liquefaction potential", *J. Soil Mech. Found. Division*, **97**(9), 1249-1273. https://doi.org/10.1061/JSFEAQ.0001662.

Seed, H.B., Tokimatsu, K., Harder, L.F. and Chung, R.M. (1985), "Influence of SPT procedures in soil liquefaction resistance evaluations", *J. Geotech. Eng.*, **111**(12),

Sonmezer Y.B., Akyuz A. and Kayabali K., (2020), "Investigation of the effect of grain size on liquefaction potential of sands", *Geomech. Eng.*, **20**(3), 243-254. https://doi.org/10.12989/gae.2020.20.3.243.

Sultana, S. and Roy, P.K. (2016), "Krill herd algorithm for optimal location of distributed generator in radial distribution system", *Appl. Soft Comput.*, **40**, 391-404. https://doi.org/10.1016/j.asoc.2015.11.036.

Terzaghi, K., Peck, R.B. and Mesri, G. (1996), *Soil Mechanics in Engineering Practice*, John Wiley & Sons, New York, USA.

Townsend, J.T. (1971), "Erratum to: Theoretical analysis of an alphabetic confusion matrix", *Perception & Psychophysics*, **10**(4), 256-256. https://doi.org/10.3758/BF03212817.

Trifunac, M. (1995), "Empirical criteria for liquefaction in sands via standard penetration tests and seismic wave energy", *Soil Dyn. Earthq. Eng*., **14**(6), 419-426. https://doi.org/10.1016/0267-7261(95)00016-N.

Whitman, R.V. (1971), "Resistance of soil to liquefaction and settlement", *Soils Found.*, **11**(4), 59-68.

Xenaki, V.C. and Athanasopoulos, G.A. (2003), "Liquefaction resistance of sand–silt mixtures: an experimental investigation of the effect of fines", *Soil Dyn. Earthq. Eng.*, **23**(3), 1-12. https://doi.org/10.1016/S0267-7261(02)00210-5.

Xue, X. and Xiao, M. (2016), "Application of genetic algorithm-based support vector machines for prediction of soil liquefaction", *Environ. Earth Sci.*, **75**(10), 874. https://doi.org/10.1007/s12665-016-5673-7.

Xue, X. and Yang, X. (2016), "Seismic liquefaction potential assessed by support vector machines approaches", *Bull. Eng. Geol. Environ.*, **75**(1), 153-162. https://doi.org/10.1007/s10064-015-0741-x.

Youd, T.L., Idriss, I.M., Andrus, R.D., Arango, I., Castro, G., Christian, J.T., Dobry, R., Finn, W.D.L., Harder, L.F., Hynes, M.E., Ishihara, K., Koester, J.P., Liao, S.S.C., Marcuson, W.F., Martin, G.R., Mitchell, J.K., Moriwaki, Y., Power, M.S., Robertson, P.K., Seed, R.B. and Stokoe, K.H. (2001), "Liquefaction resistance of soils - Summary report from the 1996 NCEER and 1998 NCEER/NSF workshops on evaluation of liquefaction resistance of soils", *J. Geotech. Geoenviron. Eng.*, **127**(4), 817-833. http://dx.doi.org/10.1061/(ASCE)1090-0241(2001)127:4(297)

Zhang, W. and Goh, A.T.C. (2016), "Evaluating seismic liquefaction potential using multivariate adaptive regression splines and logistic regression", *Geomech. Eng.*, **10**(3), 269-284. https://doi.org/10.12989/gae.2016.10.3.269.

CC

Addendix. 1 Study Data

Train Test	Lf	Mw	a_{max} (g)	D_{avg} (m)	D_{GWT} (m)	σ (kPa)	σ' (kPa)	N_{avg}	$(N1)_{60}$	FC (%)	$(N1)_{60CS}$	$K_σ$	D_r
Tr	0	6.9	0.6	2.5	1.1	43	29	27.6	40.8	10	42	1.1	97
Tr	0	7.7	0.205	2.2167	1.2	41	31	24.7	37.3	1	37.3	1.1	92
Tr	0	7.7	0.205	2.5833	1.2	48	34	14.1	23	1	23	1.1	72
Tr	0	6.5	0.12	2.5	1.2	46	34	10.1	16.2	7	16.3	1.1	61
Tr	0	6.93	0.28	2	2	35	35	18	22.6	1	22.6	1.1	71
Tr	0	6.93	0.28	2.5	1.4	45	35	16.9	21.4	5	21.4	1.1	69
Tr	0	6.9	0.6	3.5	0.9	61	36	21.2	31.6	3	31.6	1.1	84
Tr	0	6.9	0.6	3.5	0.9	63	37	26	37	0	37	1.1	91
Tr	0	7.7	0.32	3.4	0.9	63	39	19	26.2	4	26.2	1.1	77
Tr	0	7.7	0.205	2.865	1.75	52	41	12	18.7	3	18.7	1.1	65
Tr	0	6.9	0.5	3.5	1.4	61	41	20.1	29.1	6	29.2	1.1	81
Tr	0	7.7	0.205	3.42	1.2	64	42	15.9	23.5	2	23.5	1.1	73
Te	0	6.5	0.12	3.4	1.3	63	42	7	9.6	4	9.6	1.08	46
Tr	0	6.5	0.12	4.3	0.3	80	42	8	11.8	12	13.9	1.09	56
Tr	0	6.54	0.156	2.9	1.8	53	42	30.4	37.8	12	40	1.1	95
Te	0	6.53	0.78	2.9	1.8	53	42	30.4	37.8	12	40	1.1	95
Tr	0	6.9	0.6	3.5	1.7	62	44	24.2	33.5	0	33.5	1.1	87
Tr	0	8.3	0.23	4	0.9	75	45	16	23	5	23	1.1	72
Tr	0	7.7	0.205	3.5667	1.45	67	46	18.3	25.9	0	25.9	1.1	76
Tr	0	7.7	0.205	3.905	1.2	74	47	13	18.9	3	18.9	1.1	65
Tr	0	6.93	0.28	3.4	1.9	62	48	18	21.2	5	21.2	1.1	69
Tr	0	6.9	0.7	3.5	2.2	64	50	27.5	35.8	3	35.8	1.1	90
Tr	0	7.7	0.205	4.48	1.2	85	53	13.2	20.3	2	20.3	1.09	68
Tr	0	6.9	0.4	4.3	2.1	76	54	25.8	36.6	1	36.6	1.1	91
Tr	0	7.7	0.205	4.5425	1.45	86	55	15.8	23.5	2	23.5	1.09	73
Tr	0	6.5	0.12	4.3	1.8	80	56	4	5.4	10	6.5	1.05	38
Tr	0	7.7	0.2	4.5	1.4	87	57	14.2	20.9	10	22	1.08	70
Tr	0	6.9	0.6	3.5	2.8	66	59	32.5	39.7	0	39.7	1.1	95
Tr	0	7.7	0.205	5.1767	1.2	99	60	25	34.6	3	34.6	1.1	88
Tr	0	6.9	0.6	4.5	2.5	80	60	17.5	25	5	25	1.09	75
Tr	0	6.5	0.14	4	2.4	75	60	6	7.5	10	8.6	1.05	44
Tr	0	7.6	0.18	6.1	1.2	115	67	27	35	0	35.5	1.1	89
Tr	0	7.7	0.25	5	2.3	94	68	34.7	24.9	19	29.2	1.08	81
Tr	0	6.9	0.5	4.8	3.1	86	69	15	20.3	19	24.5	1.06	74
Tr	0	7.7	0.24	5.5	2.1	103	70	20	24.6	0	24.6	1.06	74
Tr	0	6.9	0.6	5	3	92	72	18.1	24	10	25.1	1.06	75
Tr	0	6.9	0.5	5.3	3.2	92	72	18.6	24.7	14	27.6	1.06	79
Tr	0	6.93	0.28	6.1	1.8	115	73	26	34.4	5	34.4	1.08	88
Tr	0	8.3	0.23	6.1	2.1	115	76	28	35.3	5	35.3	1.08	89
Tr	0	7.7	0.205	6.67	1.6	127	77	17.3	22.5	4	22.5	1.04	71
Tr	0	6.9	0.6	8.5	1.5	146	78	30.5	40.1	10	41.3	1.08	96
Tr	0	7.7	0.24	7.3	1.2	138	78	17	20.1	17	24	1.04	73
Te	0	6.5	0.14	6.1	2.4	115	79	12	14.1	3	14.1	1.03	56
Tr	0	6.9	0.6	6	2.4	114	79	30.8	38.6	6	38.6	1.07	93
Tr	0	6.9	0.4	5.2	3.5	97	80	16.6	21.1	18	25.2	1.04	75
Tr	0	7.6	0.18	7	1.8	132	81	18	22.7	2	22.7	1.03	71
Tr	0	6.9	0.5	8	2	142	83	21.3	27.9	50	33.5	1.05	87
Te	0	6.5	0.14	6.4	4.3	106	85	9	9.4	5	9.4	1.02	46
Tr	0	6.93	0.24	6.5	3	125	91	37	43.3	7	43.4	1.03	99
Tr	0	6.69	0.51	9.3	3.9	154	101	24.1	27.2	25	32.3	1	85
Tr	0	6.9	0.4	8	2.9	152	103	34.2	39.5	15	42.7	1	98
Tr	0	6.93	0.39	8.4	3	158	105	19	20.2	20	24.6	0.99	74
Tr	0	6.9	0.6	7.5	4.5	137	107	24.1	27.4	9	28	0.99	79
Tr	0	7.6	0.18	10.1	1.8	190	109	20	23.5	8	23.5	0.99	73
Tr	0	7.6	0.4	10.8	1.6	208	118	26.8	30.9	0	30.9	0.97	83

Continued-

Tr	0	6.9	0.6	7.5	6.1	137	124	20	21.3	10	22.5	0.97	71
Tr	0	6.9	0.4	8.5	5	159	125	20.2	22.7	20	27.2	0.96	78
Tr	0	6.9	0.4	9.5	5	179	135	30.9	34.6	20	39.1	0.92	94
Tr	0	6.9	0.4	10	5	189	140	18.2	19.5	20	24	0.95	73
Tr	0	6.9	0.7	10.5	7.7	199	171	40.5	42.6	0	42.6	0.85	98
Te	1	6.53	0.24	1.8	0.3	35	20	3	4.6	80	10.2	1.1	48
Tr	1	6.93	0.28	1.8	1	32	25	6.7	9.1	35	14.6	1.1	57
Te	1	6.5	0.12	2.8	0.5	53	30	4.7	6.9	5	6.9	1.1	39
Tr	1	7.7	0.32	2.8	0.5	53	30	4.7	6.9	5	6.9	1.1	39
Te	1	7.6	0.22	3.5	1.1	56	32	5.9	8.5	3	8.5	1.1	44
Te	1	6.53	0.51	2.1	1.5	38	32	3	4.6	31	10	1.1	47
Tr	1	7.7	0.24	2.5	1.2	46	34	10.1	16.2	7	16.3	1.1	61
Tr	1	7.7	0.2	4.3	1	69	37	2.6	5.1	1	5	1.08	34
Tr	1	7.7	0.25	3.5	1.7	55	38	9.8	16.2	1	16.2	1.1	60
Tr	1	7.7	0.0116	5.7	0	95	38	9	16.5	3	16.5	1.1	61
Tr	1	8.3	0.213	5.7	0	95	38	9	16.5	3	16.5	1.1	61
Tr	1	7.6	0.16	4.3	0	80	39	4	7	10	8.2	1.08	43
Tr	1	8.1	0.2	3.7	2.1	69	39	1	1.7	27	6.9	1.08	39
Tr	1	7.6	0.09	3.3	1	63	41	2.6	4.7	5	4.7	1.07	33
Tr	1	6.8	0.11	4.3	0.35	81	42	7.4	13.3	0	13.3	1.09	55
Tr	1	7.7	0.283	4.3	0.4	81	42	7.4	13.3	0	13.3	1.1	55
Tr	1	7.7	0.32	3.4	1.3	63	42	7	9.6	4	9.6	1.08	46
Tr	1	8.3	0.23	4	0.6	75	42	6	9.1	5	9.1	1.08	45
Tr	1	7.7	0.24	4.3	0.3	80	42	8	11.8	12	13.9	1.09	56
Tr	1	6.93	0.28	3	1.8	55	43	9.5	15.3	2	15.3	1.1	59
Tr	1	6.9	0.4	4	1.6	67	43	4.4	8.3	5	8.3	1.07	43
Tr	1	6.9	0.5	4.5	0.8	80	43	12.6	21.1	5	21.1	1.1	69
Tr	1	7.6	0.16	5.3	0.9	85	43	7.9	12.7	8	13	1.09	54
Tr	1	6.9	0.4	3.5	1.8	62	44	14.3	21.1	8	21.4	1.1	69
Tr	1	8.3	0.2	4	0.9	75	45	5	7.6	1	20	0.99	67
Te	1	7.7	0.2	3.5	1.4	66	45	3.7	5.5	10	6.7	1.07	39
Tr	1	6.93	0.28	3.4	1.8	61	46	6.3	10.3	1	10.3	1.07	48
Tr	1	6.9	0.4	5	1.2	84	46	7	12.1	10	13.2	1.08	54
Tr	1	6.9	0.25	4.7	0	93	46	8.5	14	20	18.5	1.1	65
Tr	1	7.6	0.16	4.6	0.6	86	47	6	9.4	0	9.4	1.07	46
Tr	1	7.7	0.24	4.3	0.9	80	47	11	15.1	0	15.1	1.08	58
Tr	1	7	0.4	4	1.2	75	48	8	11.8	0	11.8	1.07	52
Tr	1	7.7	0.205	3.7825	1.5	71	48	6	9.3	7	9.4	1.07	46
Tr	1	6.9	0.4	3.8	2	67	49	12.4	17.9	0	17.9	1.09	63
Tr	1	7.7	0.205	3.91	1.46	73	49	5.2	8.1	2	8.1	1.06	43
Tr	1	6.9	0.4	4.1	2	71	50	9.2	15	0	15	1.08	58
Te	1	6.53	0.78	3.7	1.8	68	50	2	2.9	18	7	1.06	40
Te	1	5.9	0.2	3.4	2.1	62	50	2	2.9	64	8.5	1.06	44
Te	1	6.53	0.2	3.4	2.1	62	50	2	2.9	64	8.5	1.06	44
Tr	1	6.9	0.5	3.5	2.4	63	51	18	24.6	0	24.6	1.1	74
Tr	1	7.7	0.227	7.5	0.4	123	53	7.7	12.4	1	1	1.06	15
Tr	1	7.6	0.162	3.8	2	71	53	4.5	6.8	5	6.8	1.05	39
Tr	1	7.6	0.13	4.5	1.1	87	54	9	11.7	12	13.8	1.06	56
Tr	1	6.54	0.206	4.6	1.2	87	54	7.1	10.3	30	15.7	1.07	59
Tr	1	5.9	0.26	4.6	1.2	87	54	7.1	10.3	30	15.7	1.07	59
Tr	1	6.93	0.28	3.5	2.5	65	55	13	14.9	3	14.9	1.07	58
Tr	1	6.9	0.5	4.5	2.1	79	55	12.3	18.9	6	18.9	1.08	65
Tr	1	6.9	0.35	4.7	2.2	80	55	10	15.2	20	19.6	1.08	66
Tr	1	7.7	0.205	5.21	0.72	100	56	3.3	5.4	2	5.4	1.05	35
Tr	1	7.7	0.24	4.3	1.8	80	56	4	5.4	10	6.5	1.05	38
Te	1	7.5	0.2	5.2	1.8	90	56	6	5.8	50	11.4	1.06	51
Tr	1	7.7	0.28	3.4	3.1	62	59	11	12.3	5	12.3	1.05	53
Tr	1	6.9	0.4	3.3	3.2	62	60	8	10.9	0	10.9	1.02	50
Tr	1	7.7	0.24	4	2.4	75	60	6	7.5	10	8.6	1.05	44

Continued-

Tr	1	8.1	0.2	4.3	2.4	80	61	2.3	3.4	30	8.7	1.07	44
Tr	1	6.9	0.5	6.8	1.5	114	62	5.6	8.5	5	8.5	1.04	44
Te	1	5.9	0.32	4.3	2.7	77	62	5	6.2	92	11.7	1.05	51
Tr	1	7.7	0.205	5.41	1.37	103	63	4.8	7.4	2	7.4	1.04	41
Tr	1	7.7	0.24	5.5	1.8	99	63	2	2.5	60	8.1	1.04	43
Tr	1	7.7	0.205	5.48	1.35	104	64	3.7	5.6	2	5.6	1.04	35
Tr	1	6.9	0.5	4.3	2.8	79	64	8.3	12.2	2	12.2	1.05	52
Tr	1	6.93	0.28	5.3	1.5	102	64	12	17.6	3	17.6	1.06	63
Tr	1	6.9	0.5	5	3	85	65	17.4	24.1	0	24.1	1.07	74
Tr	1	6.93	0.28	4.6	2.4	87	65	11	13.1	3	13.1	1.05	54
Tr	1	7.7	0.2	6.4	0.9	121	67	10	12.8	0	12.8	1.04	54
Tr	1	6.93	0.28	4.9	2.6	90	67	12.8	18.4	1	18.4	1.05	64
Tr	1	6.93	0.16	6.5	1.5	116	67	4.3	6.4	20	10.8	1.04	49
Te	1	7.6	0.2	6.1	0.9	118	67	9	10.5	20	15	1.05	58
Tr	1	7.7	0.205	5.7443	1.51	109	68	8	11.5	2	11.5	1.04	51
Tr	1	7.6	0.4	5.2	2	100	68	11.7	16.4	2	16.4	1.05	61
Tr	1	8.1	0.2	5.2	2.1	98	68	5.9	8.2	10	9.3	1.04	46
Tr	1	7.7	0.205	6.0356	1.58	115	71	7.3	10.2	2	10.2	1.03	48
Tr	1	7.7	0.24	5.2	2.4	98	71	9	11.1	20	15.5	1.04	59
Tr	1	7.6	0.16	7	0.9	132	72	8	9.9	2	9.9	1.03	47
Tr	1	6.9	0.4	5.9	2.3	107	72	13.4	17.8	21	22.5	1.05	71
Tr	1	6.93	0.18	5.9	3.5	97	73	4.3	5.1	50	10.7	1.03	49
Tr	1	7.7	0.205	6.47	1.46	124	74	7.3	9.9	8	10.4	1.03	48
Tr	1	6.9	0.5	6.5	2.3	116	74	9.5	12.7	15	16	1.04	60
Tr	1	6.9	0.35	5	4	89	79	15	19.3	0	19.3	1.03	66
Tr	1	7.7	0.205	6.9125	1.5	132	79	6.6	8.7	3	8.7	1.02	44
Tr	1	7.7	0.24	6.1	2.4	115	79	12	14.1	3	14.1	1.03	56
Tr	1	7.7	0.205	7.1314	1.45	136	81	10.4	13.5	3	13.5	1.02	55
Tr	1	6.9	0.5	5.7	3.7	102	82	15.1	19.2	5	19.2	1.03	66
Tr	1	7.7	0.24	6.4	4.3	106	85	9	9.4	5	9.4	1.02	46
Tr	1	7	0.3	7.8	1.5	147	85	13	13.3	48	19	1.02	65
Tr	1	7.5	0.135	10.4	1.5	139	86	6	5	3	5	1.01	34
Tr	1	6.93	0.27	6.3	3	118	86	7.5	8.6	8	9	1.01	45
Tr	1	6.69	0.43	7.1	2	139	88	7.4	8.5	64	14.1	1.02	56
Tr	1	6.93	0.28	6.3	3	121	89	14.4	15.4	3	15.4	1.01	59
Tr	1	7	0.2	8.2	1.5	155	89	9.1	7.6	67	13.2	1.01	54
Tr	1	7.7	0.25	7.2	2.3	139	90	19.9	13	19	17.3	1.01	62
Tr	1	7	0.3	8.2	1.5	158	92	11	11	5	11	1.01	50
Tr	1	6.93	0.37	6	4.5	106	92	9	10.2	8	10.6	1.01	49
Tr	1	6.9	0.5	8	3	143	94	15.1	19.1	5	19.1	1.01	66
Tr	1	6.93	0.39	6	4.4	111	95	8.8	9.8	25	14.9	1.01	58
Tr	1	6.9	0.34	7.8	2.4	149	96	5.7	6.8	20	11.3	1.01	50
Tr	1	6.61	0.45	6.1	4.6	112	96	7.3	8.1	50	13.7	1.01	56
Tr	1	6.61	0.45	6.1	4.6	112	96	3.5	3.9	55	9.5	1.01	46
Tr	1	7.6	0.16	10.1	0.9	190	100	10	11	2	11	1	50
Tr	1	6.93	0.39	6.2	4.9	114	101	9.2	9.9	32	15.3	0.99	59
Tr	1	6.69	0.51	6.7	4.3	129	105	11	11.6	33	17	1	62
Te	1	7.5	0.2	8.2	4.6	142	106	9	6.3	20	10.7	1	49
Tr	1	7.7	0.205	9.7986	1.47	189	107	5.9	6.9	4	6.9	1	39
Tr	1	6.9	0.4	7.5	4	141	107	14.8	16.8	25	21.9	0.99	70
Tr	1	6.9	0.4	8.8	3.5	166	115	10.9	12.5	2	12.5	0.99	53
Tr	1	6.9	0.35	8.9	3	173	116	5.4	6.1	1	6.1	0.9	37
Tr	1	6.9	0.34	10	3	192	123	9.7	10.8	20	15.3	0.98	59
Tr	1	6.69	0.84	8.5	7.2	156	143	13.6	13.1	50	18.7	0.96	65
Tr	1	6.9	0.34	11.5	4	219	146	12	12.3	20	16.8	0.96	61
Te	1	7.5	0.2	11.1	6.7	199	156	13	7.6	5	7.6	1	41

Appendix. 2 Validation data

No	Earthquake	Site	Depth (m)	σ' (kPa)	PGA	Mw	R (km)	N1-60	FC (%)	ΔN	Nspt-FC	Dr (%)	Cu	D50 (mm)	LF
1	Mino-Owari (1891)	Ginan	7	83	0.3	7.9	50	11.1	5	0.0	11.1	30.9	2.2	0.28	1
2	Kanto (1923)	Arakawa 7	7	125	0.2	7.9	72	10.3	10	1.2	11.5	33.4	3.4	0.25	1
3		Arakawa 7	8	144	0.2	7.9	72	3.0	14	2.1	5.1	21.5	3.4	0.25	1
4		Arakawa 12	4.3	73	0.2	7.9	72	2.7	22	4.0	6.7	21.6	45	0.18	1
5	Tohnankai (1944)	Neiko	3.5	66	0.2	8	76	1.6	27	5.1	6.7	21.3	67	0.2	1
6		Ienaga	3	51	0.2	8	76	2.9	30	5.8	8.7	23.9	7.5	0.15	1
7		Cinan	7	133	0.2	8	90	11.1	5	0.0	11.1	33.0	2.2	0.28	1
8	Fukui (1948)	Takaya2	4	36	0.4	7.2	7	11.2	35	7.0	18.2	40.6	50	0.13	0
9		Takaya2	4	68	0.4	7.3	28	11.2	35	7.0	18.2	43.9	50	0.13	0
10		Shonenji	4	76	0.4	7.3	24	11.5	o	0.0	11.5	31.3	1.4	0.45	1
11		Agri. Union	5	102	0.4	7.3	21	11.1	21	3.7	14.8	39.2	1.7	0.1	0
12	Nigata (1964)	Showa Br.2	4.3	39	0.2	7.5	65	6.2	0	0.0	6.2	17.5	1.4	0.3	1
13		Road site	6	70	0.2	7.5	35	14.6	0	0.0	14.6	37.0	1.5	0.36	0
14		River site	4.5	47	0.2	7.5	65	8.7	0	0.0	8.7	23.4	1.6	0.4	1
15		Nigata	7	133	0.2	7.5	65	9.5	2	0.0	9.5	29.8	2.5	0.3	1
16		Nigata	7	133	0.2	7.5	65	14.2	2	0.0	14.2	39.1	2.5	0.3	0
17		Nigata	7	131	0.2	7.5	65	20.3	2	0.0	20.3	50.9	2.5	0.3	0
18		Nigata	10	190	0.2	7.5	65	10.0	2	0.0	10.0	32.2	2.5	0.3	1
19		Nigata	10	190	0.2	7.5	65	16.0	2	0.0	16.0	44.0	2.5	0.3	0
20		Nigata	10	188	0.2	7.5	65	19.1	2	0.0	19.1	50.0	2.5	0.3	0
21	Tokachi-oki (1968)	Hachinohe3	4	42	0.2	7.9	65	9.1	5	0.0	9.1	23.6	3	0.25	1
22		Hachinohe4	4	46	0.2	7.9	65	23.4	5	0.0	23.4	52.1	3	0.25	0
23		Nanaehama	4	46	0.2	7.9	72	7.3	20	3.5	10.8	27.4	6	0.12	1
24		Hachinohe3	4	42	0.2	7.9	72	9.1	5	0.0	9.1	23.6	3	0.25	1
25		Hachinohe4	4	46	0.2	7.9	72	23.4	5	0.0	23.4	52.1	3	0.25	0
26	Miyagiken-oki (1978)	Nakamura5	3.3	42	0.2	7.4	44	10.6	4	0.0	10.6	26.5	2.5	0.28	1
27		Yuriagekal	5.3	60	0.2	7.4	44	2.6	60	12.8	15.4	37.9	3	0.04	1
28		Yuriageka Brl	4.3	56	0.2	7.4	44	5.4	10	1.2	6.6	20.1	4.8	0.4	1
29		Shiomi6	4	61	0.2	7.4	44	7.8	10	1.2	9.0	25.3	3.5	0.25	1
30		Nakajima2	4.5	65	0.2	7.4	44	12.6	26	4.9	17.5	42.3	12	0.12	0
31		Nakamura4	3.3	35	0.3	7.4	34	8.1	5	0.0	8.1	20.6	5	0.7	1
32		Nakamura5	3.3	42	0.3	7.4	34	10.6	4	0.0	10.6	26.5	2.5	0.28	1
33		Yuriagekal	5.3	60	0.2	7.4	44	2.6	60	12.8	15.4	37.9	2.5	0.04	1
34		Yuriage Brl	4.3	56	0.2	7.4	44	5.4	10	1.2	6.6	20.1	4.4	0.4	1
35	Miyagiken-oki (1978)	Oiiril	6.3	85	0.2	7.4	44	9.9	5	0.0	9.9	28.7	2.1	0.34	1
36		Oiiri2	6.3	72	0.2	7.4	44	9.6	4	0.0	9.6	27.3	2.6	0.36	1
37		Shiomi2	6	79	0.2	7.4	44	11.4	10	1.2	12.6	33.6	3.5	0.3	0
38		Shiomi6	4	61	0.2	7.4	44	7.8	10	1.2	9.0	25.3	3.5	0.25	1
39		Hiyori5	7	88	0.2	7.4	44	22.6	5	0.0	22.6	53.7	2.5	0.35	0
40		Nakajima2	4.5	65	0.2	7.4	44	12.6	26	4.9	17.5	42.3	12	0.12	0
41		Sendaikoul	6	73	0.2	7.4	44	17.8	11	1.4	19.2	46.2	5	0.3	0
42		Sendaikou4	7	93	0.2	7.4	44	17.7	12	1.6	19.3	47.6	5	0.3	0
43		Ishinomaki2	4	50	0.2	7.4	51	5.7	10	1.2	6.9	20.1	2	0.15	1
44		Ishinomaki 4	6	68	0.2	7.4	51	18.5	10	1.2	19.7	46.8	2.4	0.18	0
45	Izu (1978)	Mochikoshi	7	73	0.3	7	31	1.2	90	19.8	21.0	49.8	2.4	0.18	1
46	Chibakenchubu1980	Ohi	6	58	0.1	6.1	35	6.6	13	1.9	8.5	24.0	2.4	0.18	0
47		Ohi	14	108	0.1	6.1	35	3.8	27	5.1	8.9	27.8	2.4	0.17	0
48	San Francisco (1957)	Lake Merced	3	49	0.2	5.5	7	6.1	3	0.0	6.1	18.5	3	0.2	1
49	Alaska (1964)	Snow River	6	58	0.2	8.3	96	4.9	40	8.2	13.1	33.0	3	0.2	1
50		Scott Glace.	6	54	0.2	8.3	88	9.8	10	1.2	11.0	28.6	3	0.2	1
51		Valdez	6	63	0.2	8.3	56	11.9	0	0.0	11.9	31.2	3	0.2	1
52	San Fernando (1971)	Van Norman	6	88	0.5	6.6	8	6.9	20	3.5	10.4	29.8	2.4	0.1	1
53		Juvenile	6	98	0.4	6.6	10	1.4	10	1.2	3.5	16.8	2.4	0.1	1

Continued-

54		Jensen Pi.	16.5	322	0.5	6.6	8	7.4	50	10.5	17.9	49.6	2.4	0.07	1
55	Imperial Valley (1979)	Heber Rd4	4	52	0.6	6.6	3	5.6	25	4.7	10.3	27.0	11	0.12	1
56		Heber Rd7	4	52	0.6	6.6	3	15.3	19	3.3	18.6	43.3	2.4	0.1	0
57	Guatemara (1976)	Arnatitlan4	7	64	0.1	7.5	74	12.7	3	0.0	12.7	32.8	3	1	0
58	Tanshan (1976)	Lutai sı	11	130	0.2	7.8	67	7.0	50	10.5	17.5	45.4	20	0.07	1
59	Adana-Ceyhan	Büyükınangıt	5	50	0.3	6.3	4	15.1	14	2.1	17.2	40.4	3	0.02	0
60		Ceyhan	5	50	0.3	6.3	4	10.1	27	5.1	15.2	36.5	3	0.04	0
61	Kocaelil (1999)	Adapazari-A	4.6	46	0.4	7.4	27	4.5	78	16.9	21.4	48.2	3	0.04	1
62		Adapazari-Bl	2.3	23	0.4	7.4	27	3.0	88	19.3	22.3	45.9	3	0.04	1
63		Adapazari-	2	20	0.4	7.4	27	2.0	75	16.3	18.3	37.3	3	0.04	1
64		Adapazari-D	2.7	27	0.4	7.4	27	3.5	73	15.8	19.3	41.0	3	0.04	1
65		Adapazari-E	2.7	27	0.4	7.4	27	4.0	78	16.9	20.9	44.2	3	0.04	1
66		Adapazari-F	2.35	23.5	0.4	7.4	27	4.0	75	16.3	20.3	42.3	3	0.04	1
67		Adapazari-G	2.7	27	0.4	7.4	27	5.0	73	15.8	20.8	43.9	3	0.04	1
68		Adapazari-H	2.4	24	0.4	7.4	27	11.0	15	2.3	13.3	28.7	3	0.04	1
69		Adapazari-1	3.8	38	0.4	7.4	27	4.0	70	15.2	19.2	42.8	3	0.04	1
70		Adapazari-J	2.3	23	0.4	7.4	27	5.0	73	15.8	20.8	42.9	3	0.04	1
71		Adapazari-K	2.4	24	0.4	7.4	27	4.5	85	18.7	23.2	47.9	3	0.04	1
72		Adapazari-L	2.6	26	0.4	7.4	27	4.5	78	16.9	21.4	45.0	3	0.04	1
73	Roudbar 1990	Anzali	4	44	0.3	7.5	39	15.0	0	0.0	15.0	35.4	2.2	0.2	1